NOMA-Assisted On-Demand Transmissions for Monitoring Applications in Industrial IoT Networks

Ling Lyu, *Member, IEEE*, Cailian Chen, *Member, IEEE*, Nan Cheng, *Member, IEEE*, Shanying Zhu, *Member, IEEE*, Xinping Guan, *Fellow, IEEE*, and Xuemin Shen, *Fellow, IEEE*

***Abstract*—In industrial IoT networks, the critical information of monitoring applications is required to be delivered with high reliability and low latency. Moreover, different monitoring applications usually have heterogenous requirements on the transmission performance, and sensors deployed in the field to collect and deliver information are generally powered with batteries. In order to alleviate the restriction on transmission reliability, transmission capacity and energy efficiency, this paper proposes a NOMA-assisted on-demand transmission scheme for monitoring applications in industrial IoT networks. Then, an constrained optimization problem is formulated to maximum the energy efficiency under constraints of heterogenous transmission requirements and limited spectrum resources. In the solution process, the proposed scheme determines the successive interference cancellation (SIC) decoding order by taking advantage of the heterogenous requirements of different applications, which significantly reduces the solution complexity caused by the tight coupling of decoding order, power control and channel assignment. Moreover, the pairwise matching based algorithm and the minimum cost flow based algorithm is designed to solve the formulated mixed integer programming problem effectively. Finally, simulation results demonstrate that the proposed scheme could meet the transmission requirements for heterogenous monitoring applications with limited spectrum resources and has advantages on improving the energy efficiency for the industrial IoT network with battery-powered sensors.**

***Index Terms*—Industrial IoT networks, monitoring applications, heterogenous transmission requirements, spectrum limitation, NOMA-assisted transmission.**

Manuscript received February 28, 2020; revised June 9, 2020; accepted August 5, 2020. Date of publication August 31, 2020; date of current version October 22, 2020. This work was supported in part by the Fundamental Research Funds for Central Universities under Grant 3132020210, in part by Cooperative Scientific Research Project, Chunhui Program of Ministry of Education, P. R. China, in part by the Foundation of Key Laboratory of System Control and Information Processing, Ministry of Education, P. R. China, in part by the Ministry of Science and Technology of China under National Key Research and Development Project under Grant 2018YFB1702100, in part by the Natural Science Foundation of China under Grants 61933009, 61622307, and 61922058, and in part by the Shanghai Academic Research Leader under Grant 19XD1421800. The review of this article was coordinated by Dr. Y. Zhang. *(Corresponding author: Ling Lyu.)*

Ling Lyu is with the School of Information Science and Technology, Dalian Maritime University, Dalian 116026, China, and also with the Key Laboratory of System Control and Information Processing, Ministry of Education of China, Shanghai 200240, China (e-mail: linglyu@dlmu.edu.cn).

Cailian Chen, Shanying Zhu, and Xinping Guan are with the Key Laboratory of System Control and Information Processing, Ministry of Education of China, Shanghai 200240, China, and also with the Department of Automation, Shanghai Jiao Tong University, Shanghai 200240, China (e-mail: cailianchen@sjtu.edu.cn; shyzhu@sjtu.edu.cn; xpguan@sjtu.edu.cn).

Nan Cheng is with the School of Telecommunication, Xidian University, Xian 710071, China (e-mail: nancheng@xidian.edu.cn).

Xuemin Shen is with the Department of Electrical and Computer Engineering, University of Waterloo, Waterloo, ON N2L 3G1, Canada (e-mail: sshen@uwaterloo.ca).

Digital Object Identifier 10.1109/TVT.2020.3020298

I. Introduction

UBIQUITOUS situation awareness plays a crucial role in the industrial automation, where critical monitoring information is expected to be delivered reliably and timely over wireless networks. Moreover, different monitoring applications usually have heterogenous requirements on the data transmission performance [1]–[5]. For example, in the temperature-estimation application, in order to satisfy the condition of estimation convergence, the outage probability of measurements cannot exceed a certain threshold. On the other hand, the vibration monitoring of conveyance rollers (equipment-health monitoring application) concerns about the data volume obtained within the specified deadline, since the fast sample rate of vibration sensor will generate a large number of monitoring data in each control period. Thus, different industrial applications have heterogenous requirements of transmission performance.

In general, a mass of sensors are deployed in the field to obtain sufficient sensing information for industrial monitoring applications [6]–[8]. In addition, the more the sensing data of sensors are successfully got, the better the monitoring performance is [9]–[11]. In nowadays, the orthogonal multiple access (OMA) mechanism has been widely used to provide the required transmission reliability for many applications [12]–[15]. Some existing works use the OMA technique to improve the transmission reliability by assigning the dedicated resource [16]–[18]. However, these above OMA-based transmission schemes provide satisfied transmission reliability at the cost of reducing spectrum utilization and transmission capacity, which are not suitable for the industrial network with limited spectrum resources. Moreover, the sensors deployed in the field are generally powered by batteries and required to work for a long time without maintenance. If the transmission power is increased too much, the battery will be drained quickly, and thus is not practical [19]. Therefore, how to guarantee the transmission reliability to enhance the transmission capacity with the limited spectrum and energy resource is of significant importance for providing the satisfied quality of service for different monitoring applications.

The power-domain non-orthogonal multiple access (NOMA) together with the successive interference cancellation (SIC) technique makes it possible to simultaneously deliver the packets of multiple sensors on the same resource block without considerable interference [20]–[25]. Recently, the NOMA technique has been applied to facilitate the spectrum utilization improvement in existing studies [26]–[28]. Considering that NOMA-assisted

transmission could enhance the access ability and transmission performance, Refs. [29] and [30] integrated the NOMA and beamforming techniques into the considered system to increase the achievable sum rate and the number of served devices/users. Qian *et al.* [31] applied the NOMA technique into vehicular networks to enhance the long-term system-wide performance and reduce the handover rate by jointly optimizing the cell association and the power control. Diamantoulakis *et al.* [32] investigated the downlink/uplink of wireless powered networks and proposed two different NOMA protocols to fairly maximize the downlink and uplink users' rates based on the priority weights. In [33], an analytical framework for NOMA downlink and uplink multi-cell wireless systems was developed, and the system outage probability and average achievable rate were derived by using the stochastic geometry approach. Since the NOMA technique could achieve an effective interference management and improve the spectrum utilization, we employ the NOMA technique to access more sensors for multiple monitoring applications with limited spectrum.

For the NOMA-assisted transmission, this paper takes full advantage of the different requirements on transmission performance to determine the SIC decoding order, which will maintain the advantage of NOMA and reduce the complexity caused by the tight coupling of decoding order, power control and channel assignment. Furthermore, due to the error propagation in the operations of SIC, the failure in properly decoding the superimposed signals and extracting the corresponding signal of each individual sensor will increase when a larger number of devices use the same resource, especially in the circumstance of limited spectrum resources. As a solution, data packets of the same application are simultaneously delivered over different channels to mitigate the intra-application interferences. Moreover, NOMA is employed among different monitoring applications to mitigate the inter-application interferences induced by using the same resource block to deliver data packets for different applications. Based on this, this paper proposes a NOMA-assisted on-demand transmission (NDT) scheme to meet the heterogenous requirements of transmission performance for different monitoring applications. The contributions of this paper are threefold as follows.

- The proposed NDT scheme could simultaneously guarantee the transmission reliability for the temperature estimation application and improve the sum data rate for equipment-health monitoring applications with limited spectrum resource. Moreover, the NDT scheme has advantages on improving the energy efficiency for the industrial network with battery-powered sensors.
- Considering the heterogenous requirements of different applications, this paper explores the relationship between the application priority and the SIC decoding order, using which the solution complexity of joint decision of channel allocation, NOMA cluster and power control could be effectively reduced.
- The mixed interfered maximization problem is solved effectively by designing the pairwise matching based polynomial time algorithm for the two-application case and the minimum cost flow based low-complexity algorithm for the multi-application case.

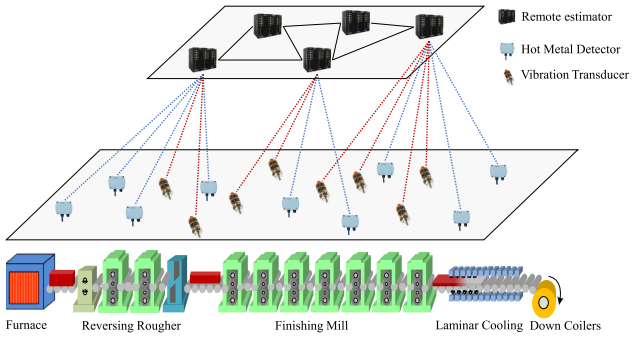

Fig. 1. Network architecture for applications in hot rolling process. (Hot metal detectors take charge to collect the temperature information and provide sensing serves for the state estimation application.Vibration transducers take charge to collect the vibration information of equipment and provide sensing serves for the equipment-health monitoring application.)

The remainder of this paper is organized as follows. The system model and the problem formulation are presented in Section II. Section III proposes and optimizes the NOMA assisted on-demand transmission scheme for industrial applications. Section IV designs the low-complexity algorithms for the on-demand transmission in the multi-application cases. Simulation results and conclusion are given in Section V and Section VI, respectively.

II. System Model and Problem Formulation

In this paper, we consider a typical paradigm of the monitoring task in industrial automation, i.e., the situation awareness for dynamic hot rolling process, as shown in Fig. 1. In order to ubiquitously perceive the physical plant, a large number of different types of sensors are deployed, e.g. hot metal detectors, vibration transducers, and so on [34]. Different types of sensors serve for different applications. Particularly, the hot metal detectors are deployed to collect the temperature information, which is then used to serve the temperature estimation application. Considering that equipment fault may make the vibrational frequency of conveyance rollers change, the vibration transducers are deployed to collect the vibration information for the equipment-health monitoring application. Moreover, different industrial applications have heterogenous requirements of transmission performance. For the temperature-estimation application, in order to satisfy the condition of estimation convergence, the outage probability of measurements cannot exceed a certain threshold. On the other hand, the vibration monitoring of conveyance rollers (equipment-health monitoring application) concerns about the data volume obtained within the specified deadline, since the fast sample rate of vibration sensor will generate a large amount of monitoring data in each control period.

A. State Estimation Based on Kalman Filter

In this paper, the considered temperature estimation application is described as a discrete-time linear system, which is expressed as

$$\mathbf{x}_{t+1} = A\mathbf{x}_t + \mathbf{w}_t, \tag{1}$$

where $\mathbf{x}_t$ is the state vector, A is the state transition matrix, and $\mathbf{w}_t \in \Re^{\kappa_x}$ is the system noise with zero mean and covariance matrix $\Xi^w \succ 0$. The initial state $\mathbf{x}_0$ is a Gaussian random vector with covariance matrix of $W_{0|0} \succ 0$. The system state is cooperatively monitored by sensors $\mathcal{S}_T$, which is expressed as

$$\mathbf{y}_{s,t} = C_s \mathbf{x}_t + \mathbf{v}_{s,t}, s \in \mathcal{S}_T, \tag{2}$$

where $\mathbf{y}_{s,t} \in \mathbb{R}^{\kappa_y}$ is the measurement cooperatively monitored by sensors $\mathcal{S}_T$, C_s is the measurement matrix, and $\mathbf{v}_{s,t} \in \mathbb{R}^{\kappa_y}$ is the observation noise with mean of $\mathbf{0}$ and covariance matrix of $\Xi_s^v \succ 0$. We consider that the tuple of (A, Ξ^w) is controllable, and the tuple of (A, C_s) is observable.

The unreliable channels and limited spectrum make the received measurements intermittent, which is modeled as a random binary variable with Bernoulli distribution $\alpha_{s,t}$ [35]. $\alpha_{s,t} = 1$ means that the measurement of the s-th sensor is received successfully. Otherwise, $\alpha_{s,t} = 0$. Let $\Pr(\alpha_{s,t} = 0)$ denote the outage probability of the raw measurements delivered by sensor $s \in \mathcal{S}$ at the end of time t. Then, the measurement equation of each sensor is

$$\widetilde{\mathbf{y}}_{s,t} = \eta_s C_s \mathbf{x}_t + \widetilde{\mathbf{v}}_{s,t}, s \in \mathcal{S}_T, \tag{3}$$

where $\widetilde{\mathbf{v}}_{s,t} = (\alpha_{s,t} - \eta_s) C_s \mathbf{x}_t + \mathbf{v}_{s,t}$ is the zero-mean white noise with covariance $\widetilde{\Xi}_{s,t}^v = \mathbb{E}\{\widetilde{\mathbf{v}}_{s,t} \widetilde{\mathbf{v}}_{s,t}^{\mathrm{T}}\} = \eta_s(1-\eta_s) \times C_s \mathbb{E}\{\mathbf{x}_{s,t} \mathbf{x}_{s,t}^{\mathrm{T}}\} C_s^{\mathrm{T}} + \Xi_{s,t}^v$, $\eta_s = \mathbb{E}\{\alpha_{s,t}\} = \Pr(\alpha_{s,t} = 1)$. According to [36], the state estimation is convergent if and only if the following condition holds:

$$\Pr(\alpha_{s,t} = 0) \leq \frac{1}{\rho^2(A)}, \tag{4}$$

where $\rho(\cdot)$ is the maximum eigenvalue of a matrix. The equation (4) shows that the transmission reliability required by the state estimation convergence. In other words, if the packet loss rate achieved by the transmission strategy is larger than $\frac{1}{\rho^2(A)}$, the state estimation is divergent. Therefore, we will investigate the transmission strategy to offer satisfactory transmission reliability for the temperature estimation application to guarantee the estimation convergence.

In addition, as the equipment-health monitoring application concerns about the data volume obtained within each control period, the sum data rate is employed to describe the requirement of this application.

B. NOMA-Assisted Transmission

In the considered scenario, there are two kinds of interferences among the sensors' transmissions, i.e., the inter-application interference which is induced by the sensors of different applications reusing the same channel, and the intra-application interference which is caused by the sensors of the same application reusing the same channel. Fortunately, the power-domain NOMA allows multiple sensors to simultaneously transmit on the same channel by employing the SIC at the remote estimator, which is beneficial for accessing more sensors and increasing the sum data rate. Considering that the large number of sensors on the same channel will increase the co-channel interference, data packets of the same application are simultaneously delivered over different channels to mitigate the intra-application interferences. Furthermore, the power control is integrated into the channel assignment to further improve the transmission reliability for the temperature estimation application and sum data rate for the equipment-health monitoring application, respectively.

In particular, take the two-application case for example. Let set $\mathcal{M}$ denote all available channels. All single-antenna field devices (such as sensors and the remote estimator) are powered with batteries. Let $p_{s,m}$ denote the transmission power of the s-th sensor on the m-th channel with the maximum p_M. In this paper, the channel gains of all channels are assumed to be independent and follow the Rayleigh block-fading model. The channel gain between the s-th sensor and the remote estimator on the m-th channel is $h_{s,m}$, which depends on the path loss and shadowing fading. The sensors deployed for temperature estimation and equipment-health monitoring applications are denoted by $\mathcal{S}_T$ and $\mathcal{S}_H$, respectively. $\delta_{s,m} = 1$ means that the m-th channel is allocated to sensor $s \in \mathcal{S}_T \cup \mathcal{S}_H$. Otherwise, $\delta_{s,m} = 0$. Without loss of generality, the cardinality of $\mathcal{S}_T$ or $\mathcal{S}_T$ is no more than that of $\mathcal{M}$. For the NOMA-assisted transmission, the following conditions should be satisfied to avoid the intra-application interference:

$$\sum_{s \in \mathcal{S}_T} \delta_{s,m} \leq 1, \tag{5}$$

$$\sum_{s' \in \mathcal{S}_H} \delta_{s',m} \leq 1. \tag{6}$$

Furthermore, in order to tackle the received signals from multiple orthogonal channels, the remote estimator adopts the maximum ratio combination (MRC) method to enhance the strength of received signal. In this case, the signal to interference plus noise ratio (SINR) out of the diversity combiner is the sum of the SINRs on each channel. Therefore, the SINR of the received signal on all assigned channels is denoted by $\Gamma_s = \sum_{m \in \mathcal{M}} \delta_{s,m} \gamma_{s,m}$, where $\gamma_{s,m}$ is the SINR for the s-th sensor on the m-th channel and the detailed expression of $\gamma_{s,m}$ is shown as Section III-A. Then, the outage probability is $\Pr(\alpha_{s,t} = 0) = \Pr\{\Gamma_s \leq \Gamma_{th}\} = \varepsilon_s$ and the achieved data rate of the s-th sensor is $\mathcal{C}_s = \log_2(1 + \Gamma_s)$. The overall transmission power of the s-th sensor is $\mathcal{P}_s = \sum_{m \in \mathcal{M}} \delta_{s,m} p_{s,m}$. Due to the outage probability, the efficient throughput is defined as the data rate of successfully transmitted information, $\mathcal{C}_s(1 - \varepsilon_s)$.

In general, higher transmission reliability leads to better estimation performance. Therefore, the sensors will increase transmission power to improve the transmission reliability of state information. However, it is not advisable to increase the transmission reliability as high as possible, especially when the transmission power of battery-powered sensor is limited and the mutual interference is heavy and complex. In this regard, the transmission scheme should guarantee the provided transmission reliability to meet the requirement of state estimation with lower power consumption. In the considered industrial IoT network, the transmission power of battery-powered sensor is limited, thus the energy efficiency [37] is regarded as a performance metric to evaluate the transmission scheme, which

is expressed as the ratio of efficient throughput and power consumption, shown as

$$\mathcal{U} = \sum_{s\in\mathcal{S}_T\cup\mathcal{S}_H} \mathcal{C}_s(1-\varepsilon_s)/\mathcal{P}_s. \tag{7}$$

C. Transmission Performance Optimization

This paper aims to maximize the energy efficiency (7) subject to the tolerable outage probability (4). The detailed problem formulation is as follows:

$$\mathrm{P}_0: \max_{\substack{\delta_{s,m}\text{'s}\in\{0,1\},\\ p_{s,m}\text{'s}\geq 0,}} \sum_{s\in\mathcal{S}_T\cup\mathcal{S}_H} \mathcal{C}_s(1-\varepsilon_s)/\mathcal{P}_s \tag{8}$$

$$\text{s.t. } \varepsilon_s \leq \frac{1}{\rho^2(A)}, \forall s\in\mathcal{S}_T, \tag{8a}$$

$$\sum_{s\in\mathcal{S}_T}\delta_{s,m}\leq 1, \forall m\in\mathcal{M}, \tag{8b}$$

$$\sum_{s\in\mathcal{S}_H}\delta_{s,m}\leq 1, \forall m\in\mathcal{M}, \tag{8c}$$

$$\sum_{m\in\mathcal{M}}\delta_{s,m}\leq 1, \forall s\in\mathcal{S}_T\cup\mathcal{S}_H, \tag{8d}$$

$$\sum_{m\in\mathcal{M}}\delta_{s,m}p_{s,m}\leq p_M, \forall s\in\mathcal{S}_T\cup\mathcal{S}_H. \tag{8e}$$

In the above problem formulation, (8a) is the relationship between the state estimation and NOMA-assisted transmission. (8b) and (8c) represent that one channel could be simultaneously used by at most two sensors of different applications. (8d) is the single-channel transmission constraint of each sensor, and (8e) is the transmission power constraint of each sensor. The network-wide revenue (7) can be improved by properly designing the channel and power allocations, i.e., jointly determining the 0-1 integer variable δ and the continuous variable p. Problem $\mathcal{P}_0$ is a mixed integer nonlinear programming.

For the general case of multiple channels, it is difficult to obtain the optimal solution of (8), since the channel-sensor mapping relationship influences the objective function, and the sensor pairing and the power allocation are influenced by the channel allocation among the sensors. In next section, we will propose an efficient low-complexity solution methodology which can achieve suboptimal yet close-to-optimal solution. A suboptimal solution is obtained by solving two sub-problem iteratively. One is the network-wide revenue optimization with given channel assignment by optimizing the power control. The other is the channel assignment among all sensors with given transmission power. This iterative process is guaranteed to converge, since both the updated transmission power and the updated channel assignment can improve the previous ones in terms of the network-wide utility while the network-wide utility is upper bounded due to the limited spectrum and energy resources.

III. Optimization of NOMA-Assisted Transmission With Channel Assignment and Power Control

The Dinkelbach method [38] is used to transform the fraction-form objective function to a polynomial form. To be specific, the maximum energy efficiency can be transformed to polynomial form with the iterative method such that $\mu_s^* = \max \mathcal{C}_s(1-\varepsilon_s)/\mathcal{P}_s$. μ_s^* is achieved, if and only if $\max\ \mathcal{C}_s(1-\varepsilon_s) - \mu_s^*\mathcal{P}_s = (\mathcal{C}_s(1-\varepsilon_s))^* - \mu_s^*\mathcal{P}_s^* = 0$, $\mathcal{C}_s(1-\varepsilon_s)\geq 0$ and $\mathcal{P}_s > 0$. For a fixed μ_s, the objective function could be rewritten as

$$\mathrm{P}_1: \max_{\substack{\delta_{s,m}\text{'s}\in\{0,1\},\\ p_{s,m}\text{'s}\geq 0,}} \sum_{s\in\mathcal{S}_T\cup\mathcal{S}_H} \mathcal{C}_s(1-\varepsilon_s) - \mu_s\mathcal{P}_s$$

$$\text{s.t. } (8\text{a}) \sim (8\text{e}) \tag{9}$$

A. Network-Wide Revenue Optimization With Power Control

We firstly consider a special case that one channel can be simultaneously used by at most two sensors of two different types. In this case, we study how to optimize the revenue for each channel with proper power control. Specifically, for each channel m, the value of pair $(\delta_{i,m}, \delta_{j,m})$ has two cases, which are elaborated as below.

1) Case 1: Assign the mth Channel to Only the Temperature Estimation Sensor, i.e., $(\delta_{i,m}, \delta_{j,m}) = (1, 0)$. In this case, $\Gamma_i = \frac{p_{i,m}|h_{i,m}|^2}{\sigma^2}$ and $p_{j,m}^* = 0$. Since $\mathcal{C}_i$ increases with the growth of decoding error probability ε_i, and moreover its first-order derivative with respect to Γ_i is positive. The maximum decoding error probability allowed by the estimation convergence is $\frac{1}{\rho^2(A)}$. In this regard, we have

$$1-\eta_i = 1-\exp\left(-\frac{\Gamma_{th}}{\Gamma_i}\right) \leq \frac{1}{\rho^2(A)},$$

which yields that the lower bound of acceptable SINR is $\underline{\Gamma}_i = \frac{\Gamma_{th}}{\ln(1+1/(\rho^2(A)-1))}$. Then, the first constraint (8a) can be rewritten as

$$p_{i,m} \geq \frac{\sigma^2\Gamma_{th}}{\ln(1+1/(\rho^2(A)-1))|h_{i=1,1}|^2}.$$

Putting all constraints into consideration, the problem in this case is formulated as

$$\mathrm{P}_2: \max_{\{p_{i,m}\text{'s}\}} \underline{\mathcal{C}}_i\big(1-1/\rho^2(A)\big) - \mu_i p_{i,m}$$

$$\text{s.t. } \frac{\sigma^2\Gamma_{th}}{\ln[1+1/(\rho^2(A)-1)]|h_{i,m}|^2} \leq p_{i,m} \leq p_M, \tag{10}$$

where $\underline{\mathcal{C}}_i = \log_2(1+\frac{p_{i,m}|h_{i,m}|^2}{\sigma^2})$. Since the objective function is unimodal, the optimal transmission power $p_{i,m}^*$ could be obtained with the golden section method [39].

2) Case 2: Assign the mth Channel to the Sensors Deployed for Both the Temperature Estimation Application and the Equipment-Health Monitoring Application Simultaneously, i.e., $(\delta_{i,m}, \delta_{j,m}) = (1, 1)$. In the NOMA-assisted transmission, the sum capacity is independent of the decoding order of the signals. However, the transmission rate of each individual sensor tightly

relies on the decoding order. For the considered two-application example, we can have

$$\gamma_{s,m}=\frac{p_{s,m}|h_{s,m}|^2}{\delta_{s,'m}\mathbb{I}_m(s,s')p_{s,'m}|h_{s,'m}|^2+\sigma^2},\, s\in\mathcal{S}_T,\, s'\in\mathcal{S}_H,$$

$$\gamma_{s,'m}=\frac{p_{s,'m}|h_{s,'m}|^2}{\delta_{s,'m}[1-\mathbb{I}_m(s,s')]p_{s,m}|h_{s,m}|^2+\sigma^2},s\in\mathcal{S}_T,s'\in\mathcal{S}_H,$$

where $\mathbb{I}_m(s,s')$ indicates the decoding order. If sensor s decodes the information in front of sensor s', then $\mathbb{I}_m(s,s')=1$. Otherwise, $\mathbb{I}_m(s,s')=0$. Moreover, the optimal decoding order is equivalent to the decreasing order of received power [40]. Based on this fact, $\mathbb{I}_m(i,j)=1$, if and only if $p_{i,m}|h_{i,m}|^2\geq p_{j,m}|h_{j,m}|^2$ and $\delta_{i,m}\delta_{j,m}=1$.

In the considered scenario, in order to meet the convergence condition of state estimation with intermittent measurements, the slab-temperature estimation application has higher requirements on the transmission reliability compared with the equipment-health monitoring application. In this case, the temperature monitoring sensor has higher priority than the equipment-health monitoring sensor, which motivates us to assume that the jth equipment-health monitoring sensor is decoded before the ith temperature monitoring sensor, i.e., the received power should satisfy the condition that

$$p_{j,m}|h_{j,m}|^2\geq p_{i,m}|h_{i,m}|^2.$$

As a result, for sensor $i\in\mathcal{S}_T$, there exists $\gamma_{i,m}=\frac{p_{i,m}|h_{i,m}|^2}{\sigma^2}$. For the jth sensor, the achievable SINR of received signal is $\gamma_{j,m}=\frac{p_{j,m}|h_{j,m}|^2}{p_{i,m}|h_{i,m}|^2+\sigma^2}$. In order to guarantee the estimation convergence, the decoding error probability of the ith sensor should not exceed $\frac{1}{\rho^2(A)}$. Under this circumstance, we adjust the transmission power $p_{i,m}$ and $p_{j,m}$ to maximize $\mathcal{U}$ while meeting the following condition

$$1-\exp\left(-\frac{\Gamma_{th}\sigma^2}{p_{i,m}|h_{i,m}|^2}\right)\leq\varepsilon_i\leq\frac{1}{\rho^2(A)}.$$

Since the transmission parameters of the j-th sensor does not affect the achieved transmission rate of the i-th sensor, the transmission power $p_{i,m}$ is firstly adjusted the following optimization problem:

$$\begin{aligned}\mathrm{P}_3:\ \max_{\{p_{i,m}\text{'s}\}}\ & \mathcal{C}_i\left(1-\exp\left(-\frac{\Gamma_{th}\sigma^2}{p_{i,m}|h_{i,m}|^2}\right)\right)-\mu_i p_{i,m}\\ \text{s.t.}\ \ & 1-\exp\left(-\frac{\Gamma_{th}\sigma^2}{p_{i,m}|h_{i,m}|^2}\right)\leq\frac{1}{\rho^2(A)},\forall i\in\mathcal{S}_T,\end{aligned}\quad(11)$$

where the range of transmission power is $\frac{\Gamma_{th}\sigma^2}{|h_{i,m}|^2}\leq p_{i,m}\leq\hat{p}_M$. Furthermore, the lower bound of $p_{i,m}$ could be obtained based on the equation $1-\exp(-\frac{\Gamma_{th}\sigma^2}{p_{i,m}|h_{i,m}|^2})=\frac{1}{\rho^2(A)}$. It yields

$$p_{i,m}^{\mathrm{LB}}=\min\left\{\frac{\Gamma_{th}\sigma^2}{|h_{i,m}|^2},\frac{\Gamma_{th}\sigma^2}{[\ln(\rho^2(A))-\ln(\rho^2(A)-1)]|h_{i,m}|^2}\right\}.$$

We then search the optimal $p_{i,m}^*$ in terms of maximizing (11) with the golden section method in the range of $[p_{i,m}^{\mathrm{LB}},\hat{p}_M]$. With given $p_{i,m}^*$ and $\mathcal{C}_i^*$, the maximum network-wide revenue could be obtained by

$$\begin{aligned}\mathrm{P}_4:\ \max_{\{p_{j,m}\text{'s}\}}\ & \mathcal{C}_j(1-\varepsilon_j)-\mu_j p_{j,m}+\mathcal{C}_i^*(1-\varepsilon_i)-\mu_i p_{i,m}^*\\ \text{s.t.}\ \ & p_{j,m}|h_{j,m}|^2\geq p_{i,m}^*|h_{i,m}|^2,\forall j\in\mathcal{S}_H,\end{aligned}\quad(12)$$

which could be solved with the same method that is used to solve problem (11).

B. Channel Assignment Among Sensors Deployed for Different Applications

In the general case with multiple channels and two arbitrary kinds of applications, once the matching relationship between sensor-pairs and channels is known, the transmission powers of sensors working on each channel can be determined by the solution procedure provided in Section III.A. As a consequence, the next step is to investigate the three-dimension pairing problem to determine the matching relationship (m,i,j) between channel $m\in\mathcal{M}$ and a sensor $i\in\mathcal{S}_T$ used for slab-temperature estimation, and a sensor $j\in\mathcal{S}_H$ used for equipment-health monitoring. Our objective is to find the optimal matching to maximize the network-wide energy efficiency under the given transmission power. In order to provide high transmission performance for ensuring the estimation convergence, sensor $j\in\mathcal{S}_H$ is decoded before sensor $i\in\mathcal{S}_T$ (i.e., the decoding order indicator $\mathbb{I}_m(i,j)=0$), when the channel m is occupied by two kinds of sensors. Thus, the following requirement is needed

$$p_{j,m}|h_{j,m}|^2\geq p_{i,m}|h_{i,m}|^2,i\in\mathcal{S}_T,j\in\mathcal{S}_H,\quad(13)$$

since the decoding order at the receiver in the uplink transmission depends on the strength of received signal. In order to guarantee the successful decoding for two kinds of sensors, the transmission power should satisfy the following two constraints:

$$\frac{(\sigma^2+p_{i,m}|h_{i,m}|^2)\underline{\Gamma}_i}{|h_{j,m}|^2}\leq p_{j,m}\leq p_M,j\in\mathcal{S}_H,$$

$$\frac{\sigma^2\underline{\Gamma}_i}{|h_{i,m}|^2}\leq p_{i,m}\leq p_M,i\in\mathcal{S}_T.$$

For the special case in which the channel m is allocated to only sensor $i\in\mathcal{S}_T$, the transmission power range is also $\frac{\sigma^2\underline{\Gamma}_i}{|h_{i,m}|^2}\leq p_{i,m}\leq p_M$. Similarly, if the channel m is allocated to only sensor $j\in\mathcal{S}_H$, the transmission power range is $\frac{\sigma^2\underline{\Gamma}_i}{|h_{j,m}|^2}\leq p_{j,m}\leq p_M$. Taking the estimation convergence into consideration, the initialization of transmission power for sensor $i\in\mathcal{S}_T$ is given by $\hat{p}_{i,m}=\frac{\sigma^2\underline{\Gamma}_i}{|h_{i,m}|^2}$. In this case, the initialization of transmission power for sensor $j\in\mathcal{S}_H$ is expressed as $\hat{p}_{j,m}=\frac{\sigma^2(1+\underline{\Gamma}_i)\underline{\Gamma}_i}{|h_{j,m}|^2}$. The original problem $\mathcal{P}_0$ with the given transmission powers ($\hat{p}_{i,m}$ and $\hat{p}_{i,m}$) is transformed into a binary programming problem.

$$\mathcal{P}_5: \max_{\{\delta_{s,m}\text{'s}\in\{0,1\}\}} \sum_{s\in\mathcal{S}} \mathcal{C}_s(1-\varepsilon_s) - \sum_{s\in\mathcal{S}} \mu_s \left(\sum_{m\in\mathcal{M}} \delta_{s,m}\hat{p}_{s,m}\right) \quad (14)$$

$$\text{s.t. } \varepsilon_i \le \frac{1}{\rho^2(A)}, \forall i \in \mathcal{S}_T, \quad (14a)$$

$$\sum_{i\in\mathcal{S}_T} \delta_{i,m} \le 1, \forall m \in \mathcal{M}, \quad (14b)$$

$$\sum_{j\in\mathcal{S}_H} \delta_{j,m} \le 1, \forall m \in \mathcal{M}, \quad (14c)$$

$$\sum_{m\in\mathcal{M}} \delta_{s,m} \le 1, \forall s \in \mathcal{S}_T \cup \mathcal{S}_H. \quad (14d)$$

Since each sensor can obtain at most one channel, we have $\log_2(1+\sum_{m\in\mathcal{M}} \delta_{s,m}\gamma_{s,m}) = \sum_{m\in\mathcal{M}} \delta_{s,m} \log_2(1+\gamma_{s,m})$, and moreover, the objective function of (14) decreases when ε_s increases. As a consequence, the inequality constraint (14a) becomes equality, when the objective function is maximized. In the considered scenario, we consider that there are more sensors than spectrum resources, i.e., $S_T + S_H > M$.

However, in practice, it is challenging to ensure that the packets of all sensors in set $\mathcal{S}_T$ are always decoded before those of the sensors belonged set $\mathcal{S}_H$ on all channels. Therefore, we will focus on solving this three-dimensional assignment problem directly. Define a new three-dimensional binary variable $\theta_{i,j,m} = \delta_{i,m}\delta_{j,m}$, and its corresponding utility function is given by:

$$\theta_{i,j,m}\mathcal{Q}_{i,j,m} + (1-\theta_{i,j,m})(\delta_{i,m}\mathcal{Q}_{i,m} + \delta_{j,m}\mathcal{Q}_{j,m}), \quad (15)$$

$$\mathcal{Q}_{i,j,m} = \log_2(1+\hat{\gamma}_{i,m})\left(1-\frac{1}{\rho^2(A)}\right) + \frac{1}{2}\log_2(1+\hat{\gamma}_{j,m}) - (\mu_i\hat{p}_{i,m} + \mu_j\hat{p}_{j,m}) \quad (15a)$$

$$\mathcal{Q}_{i,m} = \log_2(1+\hat{\gamma}_{i,m})\left(1-\frac{1}{\rho^2(A)}\right) - \mu_i\hat{p}_{i,m} \quad (15b)$$

$$\mathcal{Q}_{j,m} = \frac{1}{2}\log_2(1+\hat{\gamma}_{j,m}) - \mu_j\hat{p}_{j,m}. \quad (15c)$$

When $\theta_{i,j,m} = 1$ and $\hat{p}_{i,m}|h_{i,m}|^2 \ge \hat{p}_{j,m}|h_{j,m}|^2$, it yields that $\mathbb{I}_m(i,j) = 1$, $\hat{\gamma}_{i,m} = \frac{\hat{p}_{i,m}|h_{i,m}|^2}{\hat{p}_{j,m}|h_{j,m}|^2+\sigma^2}$ and $\hat{\gamma}_{j,m} = \frac{\hat{p}_{j,m}|h_{j,m}|^2}{\sigma^2}$. On the contrary, if $\hat{p}_{i,m}|h_{i,m}|^2 < \hat{p}_{j,m}|h_{j,m}|^2$, we can obtain that $\mathbb{I}_m(i,j) = 0$, $\hat{\gamma}_{i,m} = \frac{\hat{p}_{i,m}|h_{i,m}|^2}{\sigma^2}$ and $\hat{\gamma}_{j,m} = \frac{\hat{p}_{j,m}|h_{j,m}|^2}{\hat{p}_{i,m}|h_{i,m}|^2+\sigma^2}$. Based on the above result, once the variable $\theta_{i,j,m}$ is determined, we can determine the decoding order for each channel based on the transmission power and channel gain. According to (15), the problem (14) is transformed to

$$\mathcal{P}_6: \max_{\substack{\delta_{i,m}\text{'s}\in\{0,1\},\\ \delta_{j,m}\text{'s}\in\{0,1\},\\ \theta_{i,j,m}\text{'s}\in\{0,1\}}} \sum_{i\in\mathcal{S}_T}\sum_{j\in\mathcal{S}_H}\sum_{m\in\mathcal{M}} \{\theta_{i,j,m}\mathcal{Q}_{i,j,m} + (1-\theta_{i,j,m})(\delta_{i,m}\mathcal{Q}_{i,m} + \delta_{j,m}\mathcal{Q}_{j,m})\} \quad (16)$$

$$s.t. \sum_{i\in\mathcal{S}_T} \delta_{i,m} \le 1, \forall m \in \mathcal{M}, \quad (16a)$$

$$\sum_{j\in\mathcal{S}_H} \delta_{j,m} \le 1, \forall m \in \mathcal{M}, \quad (16b)$$

$$\sum_{m\in\mathcal{M}} \delta_{i,m} \le 1, \forall i \in \mathcal{S}_T, \quad (16c)$$

$$\sum_{m\in\mathcal{M}} \delta_{j,m} \le 1, \forall j \in \mathcal{S}_H, \quad (16d)$$

$$\theta_{i,j,m} = \delta_{i,m}\delta_{j,m}. \quad (16e)$$

C. Low-Complexity Algorithm for Channel Assignment

The reconstructed problem (16) is a mixed binary nonlinear programming problem, and thus, the optimal solution can be obtained by using the branch-and-bound method with the cost of high computation complexity (especially when the number of channels and sensors are large). In order to overcome this challenge, a pairwise matching-based greedy algorithm is designed for the case with multiple channels. This motivates us to propose a low-complexity greedy algorithm (called as low-complexity channel assignment (LCCA)) to determine the values of $\theta_{i,j,m}$ with given transmission power. The LCCA algorithm is constituted of three sub-procedures. Subprocedure-I aims to determine the best sensor-pair for each channel. In this way, a sensor may be assigned to more than one channel. Thus, Subprocedure-II is further performed to determine the best channel for each single-channel sensor. After that, Subprocedure-III is designed to check whether there are unassigned but available channels. As $\mathcal{Q}_{i,j,m}$ monotonically increases with the growth of $\hat{\gamma}_{i,m}$ and/or $\hat{\gamma}_{j,m}$, it is employed to evaluate the contribution of channel m to the objective function of (16). How to determine the three-dimensional matching relationship is elaborated in Algorithm 1.

In Subprocedure-I, initialize the candidate list ℓ_m for each channel $m \in \mathcal{M}$ by sorting all sensor-pairs in the descending order of $\mathcal{Q}_{i,j,m}, \forall i \in \mathcal{S}_T, \forall j \in \mathcal{S}_H$ (Step 4). Then, number the channels in the descending order of the first element in the list ℓ_m (Step 5). For each of the maximum m elements in list ℓ_m, extract the coordinates $(i_m^*, j_m^*) = \arg\max_{\{i\in\mathcal{S}_T, j\in\mathcal{S}_H\}} \mathcal{Q}_{i,j,m}$ and then add it into the candidate set $\mathcal{C}_m \leftarrow (i_m^*, j_m^*)$ (Step 9). It means that channel m is allocated to the sensor-pair (i_m^*, j_m^*), which is mathematically denoted by $\theta_{i_m^*, j_m^*, m} = 1$. In order to ensure that other channels are no longer assigned to this sensor-pair (i_m^*, j_m^*), remove i^* and j^* from $\mathcal{S}_T$ and $\mathcal{S}_H$ and $\mathcal{M}$, respectively. This operation of element remove is mathematically denoted by the set update, i.e., $\mathcal{S}_T \leftarrow \mathcal{S}_T \backslash i^*$ and $\mathcal{S}_H \leftarrow \mathcal{S}_H \backslash j^*$ (Step 10).

In Subprocedure-II, we firstly find out the elements in set $\mathcal{C}$ with $i_{m'}^* = i_m^*$ or $j_{m''}^* = j_m^*$, and the maximum sensor-pair in terms of $\mathcal{Q}_{i_m, j_m, m}$. The number of selected elements will not exceed two. For notation simplicity, let

$$(i_{m'}^-, j_{m'}^*, m') = \arg \max_{\{i\in\mathcal{S}_T\backslash i_m^*, j\in\mathcal{S}_H\}} \mathcal{Q}_{i_m, j_m, m'}, \quad (17)$$

$$(i_{m''}^*, j_{m''}^-, m'') = \arg \max_{\{i\in\mathcal{S}_T, j\in\mathcal{S}_H\backslash j_m^*\}} \mathcal{Q}_{i_m, j_m, m''}, \quad (18)$$

$$(i_m^-, j_m^-, m) = \arg \max_{\{i\in\mathcal{S}_T\backslash i_{m'}^*, j\in\mathcal{S}_H\backslash j_{m''}^*\}} \mathcal{Q}_{i_m, j_m, m}. \quad (19)$$

Algorithm 1: LCCA.

1: **Input:** The sets of each kind of sensors $\mathcal{S}_T$ and $\mathcal{S}_H$, transmission power $\hat{p}_{i,m}$ and $\hat{p}_{j,m}$ for sensors i and j, the corresponding SNRs $\hat{\gamma}_{i,m}$ and $\hat{\gamma}_{j,m}$;
2: **Output:** Three-dimensional matching relationship θ;
3: **Initialize:** Utilization matrix $\mathcal{Q}$ based on (15a)-(15c), and channels used by all sensor-pairs $\mathcal{M}_{triple} = \emptyset$;

Subprocedure-I: Determine the best sensor-pair for each channel

4: Build the candidate sensor-pair list ℓ_m for each channel $m \in \mathcal{M}$ by sorting all sensor-pairs in the descending order of $\mathcal{Q}_{i,j,m}$;
5: Number the channel in the descending order of the first element in the sensor-pair list (i,e, $\ell_m[1]$);
6: **for** Each channel $m \in \mathcal{M}$ **do**
7: $(i_m^*, j_m^*) = \arg\max_{\{i\in\mathcal{S}_T, j\in\mathcal{S}_H\}} \mathcal{Q}_{i,j,m}$;
8: **if** $i_m^* \neq i_{m'}^*$ and $j_m^* \neq j_{m'}^*$ $(m' \in \{1, \cdots, m-1\})$ **then**
9: $\theta_{i_m^*, j_m^*, m} = 1$ and $\mathcal{C}_m \leftarrow (i_m^*, j_m^*)$;
10: $\mathcal{S}_T \leftarrow \mathcal{S}_T \backslash i^*$ and $\mathcal{S}_H \leftarrow \mathcal{S}_H \backslash j^*$;
11: $\mathcal{M}_{triple} \leftarrow \mathcal{M}_{triple} \cup m$;
12: **else**
13: Subprocedure-II;
14: **end if**
15: **end for**

Subprocedure-II: Update overlapped sensor-pairs

16: Obtain the coordinates $(i_{m'}^-, j_{m'}^*, m')$, $(i_{m''}^*, j_{m''}^-, m'')$, (i_m^-, j_m^-, m) based on (17)–(19);
17: **if** $\{\mathcal{Q}_{i_m^*, j_m^*, m} + \mathcal{Q}_{i_{m'}^-, j_{m'}^*, m'} + \mathcal{Q}_{i_{m''}^*, j_{m''}^-, m''} > \mathcal{Q}_{i_m^-, j_m^-, m} + \mathcal{Q}_{i_{m'}^*, j_{m'}^*, m'} + \mathcal{Q}_{i_{m''}^*, j_{m''}^*, m''}\}$ **then**
18: $\theta_{i_m^*, j_m^*, m} = 1$, $\theta_{i_{m'}^*, j_{m'}^*, m'} = 0$, $\theta_{i_{m''}^*, j_{m''}^*, m''} = 0$;
19: $\theta_{i_{m'}^*, j_{m'}^*, m'} = \theta_{i_{m'}^-, j_{m'}^*, m'} = 1$; $\theta_{i_{m''}^*, j_{m''}^*, m''} = \theta_{i_{m''}^*, j_{m''}^-, m''} = 1$;
20: **else**
21: $\theta_{i_m^*, j_m^*, m} = \theta_{i_m^-, j_m^-, m} = 1$;
22: **end if**
23: **return** $\mathcal{Q}_{triple} = \sum_{m\in\mathcal{M}_{triple}} \mathcal{Q}_{i_m^*, j_m^*, m}$;

Subprocedure-III: Reassign remaindering channels

24: **while** $|\mathcal{M}_{triple}| < |\mathcal{M}|$ **do**
25: **if** $\mathcal{S}_T \neq \emptyset$ **then**
26: $i_m^* = \arg\max_{\{i\in\mathcal{S}_T\}} \mathcal{Q}_{i,m}$;
27: $\delta_{i_m^*, m} = 1$, $\mathcal{M}_{triple} \leftarrow \mathcal{M}_{triple} \cup m$;
28: **else**
29: **if** $\mathcal{S}_H \neq \emptyset$ **then**
30: $j_m^* = \arg\max_{\{j\in\mathcal{S}_H\}} \mathcal{Q}_{j,m}$;
31: $\delta_{j_m^*, m} = 1$, $\mathcal{M}_{triple} \leftarrow \mathcal{M}_{triple} \cup m$;
32: **else**
33: $(i_m^\dagger, j_m^\dagger, m^\dagger) = \arg\min_{\theta_{i,j,m}=1} Q_{i,j,m}$, $\theta_{i_m^\dagger, j_m^\dagger, m^\dagger} = 0$;
34: $\mathcal{M}_B \leftarrow \mathcal{M} \backslash \mathcal{M}_{triple} \cup m^\dagger$;
35: $\mathcal{S}_T \leftarrow \mathcal{S}_T \cup i_m^\dagger$, $\mathcal{S}_H \leftarrow \mathcal{S}_H \cup j_m^\dagger$;
36: $(i_m^\dagger, j_m^\dagger) = \arg\max_{\{i\in\mathcal{S}_T, j\in\mathcal{S}_H\}} \mathcal{Q}_{i,m} + \mathcal{Q}_{j,m}, \forall m \in \mathcal{M}_B$;
37: $\delta_{i_m^\dagger, m} = 1$, $\delta_{j_m^\dagger, m} = 1$;
38: **end if**
39: **end if**
40: $\mathcal{Q}_{dual} = \mathcal{Q}_{dual} + \sum_{m\in\mathcal{M}_B} (\mathcal{Q}_{i_m^\dagger, m} + \mathcal{Q}_{j_m^\dagger, m})$;
41: **end while**
42: **return** $\mathcal{Q}_{total} = \mathcal{Q}_{triple} + \mathcal{Q}_{dual}$.

a sensor may be assigned to more than one channel, thus SubProcedure-II is performed to determine the best channel for the single-channel sensor. Then, deal with the problem of overlapped sensor-pairs (Step 17-Step 22). The channel m will be allocated to the sensor-pair (i_m^*, j_m^*), if the condition $\mathcal{Q}_{i_m^*, j_m^*, m} + \mathcal{Q}_{i_{m'}^-, j_{m'}^*, m'} + \mathcal{Q}_{i_m^*, j_{m'}^-, m''} > \mathcal{Q}_{i_m^-, j_m^-, m} + \mathcal{Q}_{i_{m'}^*, j_{m'}^*, m'} + \mathcal{Q}_{i_{m''}^*, j_{m''}^*, m''}$ is satisfied. Otherwise, channel m is assigned to sensor pair (i_m^-, j_m^-). In addition, channels m' and m'' are allocated to sensor-pairs $(i_m^*, j_{m'}^-)$ and $(i_{m'}^-, j_m^*)$, respectively. At last, return the set of channels used by all sensor-pairs $\mathcal{M}_{triple}$ and the achieved utilization $\mathcal{Q}_{triple} = \sum_{m=1}^{M_{triple}} \mathcal{Q}_{i_m^*, j_m^*, m}$ (Step 23).

In SubProcedure-III, if the number of sensor-pairs is less than that of all available channels (i.e., $|\mathcal{M}_{triple}| < |\mathcal{M}|$), the residual channels are firstly assigned to only one sensor in set $\mathcal{S}_T$ (Step 25–Step 27). After that, if $\mathcal{S}_T = \emptyset$ and $\mathcal{S}_H \neq \emptyset$, each channel in set $\mathcal{M} - \mathcal{M}_{triple}$ is assigned to only one sensor in set $\mathcal{S}_H$ (Step 29-Step 31). If there are still some remaining channels when $\mathcal{S}_T = \emptyset$ and $\mathcal{S}_H = \emptyset$, break up some sensor-pairs and assign to each sensor a channel to improve the transmission performance by avoiding the co-channel interference. In particular, select the already built three-dimensional matching pair $(i^\dagger, j^\dagger, m^\dagger)$ with minimum utility $Q_{i,j,m}$. Then, break up the sensor-pair $(i^\dagger, j^\dagger)$ and let $\theta(i^\dagger, j^\dagger, m^\dagger) = 0$ (Step 33). Finally, select the best two channels in set $\mathcal{M}_B = \mathcal{M} \backslash \mathcal{M}_{triple} \cup m^\dagger$ for sensors $i^\dagger$ and $j^\dagger$ in terms of maximizing $(\mathcal{Q}_{i,m} + \mathcal{Q}_{j,m})$ (Step 36). The reassigning procedure continues until all available channels have been used. At the end of three sub-procedures, the three-dimensional matching problem has been solved with the proposed algorithm, whose performance is evaluated by comparing with the two-dimensional assignment algorithm based on the allocation of channels to each kind of sensors.

For the sake of notation simplicity, define the input size as $Z = \max\{|\mathcal{S}_T|, |\mathcal{S}_H|, |\mathcal{M}|\}$ during the complexity analysis. In SubProcedure-I, the main part of time complexity is the sorting operation in Step 4, which is $\mathcal{O}(Z^2 \log(Z))$. To be specific, the time complexity of Step 5 is $\mathcal{O}(Z \log(Z))$, and the conditional statements (Step 9-Step 11) will be executed at most Z times. In SubProcedure-II, the time complexity of updating overlap matching pairs for all channels is $\mathcal{O}(Z)$, and thus the time complexity of the for-loop is $\mathcal{O}(Z)$. In SubProcedure-III, the while-loop will be executed at most $|\mathcal{M} - \mathcal{M}_{triple}|$ times, which is less than Z. Therefore, the time complexity of reassigning remaindering channels is $\mathcal{O}(Z)$. In summary, the overall time complexity of the proposed algorithm is $\mathcal{O}(Z^2 \log(Z))$, indicating that it is a polynomial time algorithm. For easy to follow, the diagram of detailed solution process, as shown in Fig. 2. In particular, the Dinkelbach method is used to transform the fraction-form objective function in the original problem P_0 to a polynomial form, and the transformed problem is expressed as P_1. Considering P_1 as a mix-integer nonlinear programming problem, the near optimal solution is obtained by iteratively solving two sub-problems. One is to optimize the transmission power to improve the network-wide revenue by power control, and the other is the channel assignment with given transmission power.

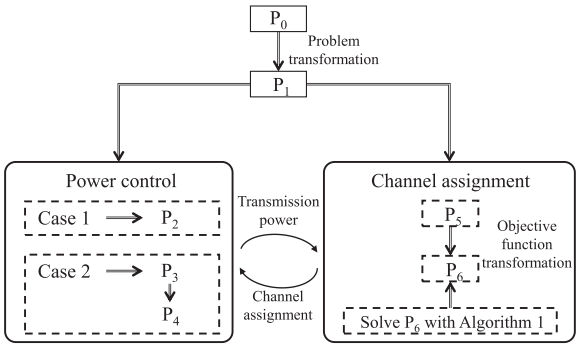

Fig. 2. The diagram of solution process.

IV. Multiple Applications With Graph-Based Minimum Cost Flow Method

In this section, we consider more general cases that involve multiple applications and each application consists of multiple sensors. In these cases, the time complexity of aforementioned LCCA algorithm is exponential-time, i.e., $\mathcal{O}(Z^{(Z+1)}\log(Z))$. We adopt the network flow technique to solve the problem of channel assignments among multiple kinds of sensors deployed for different applications.

A. Preliminaries About the Graph-Based Minimum Cost Flow

The minimum cost flow is usually mathematically formulated with a directed graph $\mathcal{G}=\{\mathcal{V},\mathcal{W}\}$, where $\mathcal{V}$ is a set of V nodes, and $\mathcal{W}$ is a set of W directed arcs [41]. Let $\varpi[\kappa,\kappa']$ denote the arc from node κ to node κ' and $\chi(\varpi[\kappa,\kappa'])$ denote the flow on the arc $\varpi[\kappa,\kappa']$. Each arc $\varpi\in\mathcal{W}$ has an associated cost $\mathcal{C}(\varpi)$, which denotes the cost of per unit flow. Then, the total cost of a flow χ is expressed as $\sum_{\varpi\in\mathcal{W}}\mathcal{C}(\varpi)\chi(\varpi)$, which is the objective function of the minimum cost flow problem. Each arc should meet the capacity constraint, i.e., $\mathcal{B}^-(\varpi)\le\chi(\varpi)\le\mathcal{B}^+(\varpi)$, where the upper bound $\mathcal{B}^-(\varpi)$ and the lower bound $\mathcal{B}^+(\varpi)$ denote the maximum and minimum amounts that can flow on the arc ϖ, respectively. Moreover, each arc is associated with $\beta(\kappa)$, and the sign of $\beta(\kappa)$ denotes the role of node in the network. In particular, $\beta(b)>0$ denotes that the amount of flow is generated from the source node b, while $\beta(d)<0$ denotes that the amount of flow is destroyed at the sink node d. Besides, $\beta(\kappa)=0$ denotes that $\kappa\in\mathcal{V}\backslash\{b,d\}$ acts as the intermediate node. In short, the minimum flow problem, whose main idea is to determine a flow from the source node to the sink node with the objective of minimizing the total cost under the condition of satisfying the capacity and divergence constraints.

B. Graph Construction for the Channel Assignment Problem

Our considered channel assignment problem among multiple applications with different-priority sensors can be modeled as the minimum cost flow problem. In the considered scenario with multiple different-priority applications, all applications in set $\mathcal{K}$ are sorted in the decreasing order in terms of priority. The higher transmission reliability the application requires, the higher priority the application has. Moreover, a set of sensors $\mathcal{S}_k(k\in\mathcal{K})$ are deployed to provide service for the k-th application. In this case, the vertex set in graph constructed for the k-th application is $\mathcal{V}_k=\mathcal{M}\bigcup\mathcal{S}_k\bigcup\{b,d\}$. The number of nodes in the built graph is $|\mathcal{V}_k|=MS_k+2$. Each arc in the graph represents the association between channels and sensors, whose capacity bounds is defined as $\mathcal{B}^-(\varpi)=0$ and $\mathcal{B}^+(\varpi)=1$. It means that $0\le\chi_k(\varpi)\le1$, and the value of $\chi_k(\varpi)$ is an integer. If there exists a flow on the arc between channel m and sensor i_k in the k-th graph, $\chi_k(\varpi[m,i_k])=1$. Otherwise, $\chi_k(\varpi[m,i_k])=0$. The cost $\mathcal{C}_k(\varpi)$ is related to its starting point and ending point, which is elaborated as follows:

- The arc $\{\varpi[b,m]|m\in\mathcal{M}\}$ starts from the source node and ends at the intermediate node, whose cost is defined as $\mathcal{C}_k(\varpi[b,m])=0$ by regarding it as a virtual connection.
- The arc $\{\varpi_{m,i_k}|m\in\mathcal{M},i_k\in\mathcal{S}_K\}$ starts from the intermediate node and ends at the intermediate node, whose cost is defined as $\mathcal{C}_k(\varpi[m,i_k])=-\mathcal{U}_{i_k,\underline{\mathcal{S}}_k,m}$. In particular, $\mathcal{U}_{i_k,\underline{\mathcal{S}}_k,m}$ denotes the achieved utility for the k-th application,

$$\mathcal{U}_{i_k,\underline{\mathcal{S}}_k,m}=\log_2(1+\hat{\gamma}_{i_k,\underline{\mathcal{S}}_k,m})(1-\varepsilon_{i_k})-\mu_{i_k}\hat{p}_{i_k,m}, \quad (20)$$

  with $\hat{\gamma}_{i_k,\underline{\mathcal{S}}_k,m}=\frac{\hat{p}_{i_k,m}|h_{i_k,m}|^2}{\sum_{k'=1}^{k-1}\sum_{j\in\mathcal{S}_{k'}}\chi_{k'}(\varpi[m,j_{k'}])\hat{p}_{j_{k'},m}|h_{j_{k'},m}|^2+\sigma^2}$.
- The arc $\{\varpi_{i_k,d}|i_k\in\mathcal{S}_K\}$ starts from the intermediate node and ends at the sink node, whose cost is defined as $\mathcal{C}_k(\varpi[i_k,d])=0$ by regarding it as a virtual connection.

Note that the values of $\chi_{k'}(\varpi)(k'\in\{1,\cdots,k-1\})$ are known when solving the minimum flow problem for the k-th application. Therefore, we can get the values of achieved utility $\mathcal{U}_{i_k,\underline{\mathcal{S}}_k,m}$ and cost $\mathcal{C}_k(\varpi)$. Without loss of generality, we assume that the maximum allowable number of transmitters on the same resource unit is K_0, due to the error propagation of the SIC.

C. Channel Assignment in the Case With Multiple Applications

After the graph construction, the revenue optimization for the k-th application is mathematically expressed as

$$\mathcal{P}_k:\min_{\chi_k}\sum_{\varpi\in\mathcal{W}}-\mathcal{U}_{i_k,\underline{\mathcal{S}}_k,m}\chi_k(\varpi[m,i_k]) \quad (21)$$

$$s.t.\ 0\le\chi_k(\varpi[m,i_k])\le1,\forall m\in\mathcal{M},\forall i_k\in\mathcal{S}_k, \quad (21a)$$

$$\chi_k(\varpi[b,m])+\sum_{i_k\in\mathcal{S}_K}\chi_k(\varpi[m,i_k])=0,\forall m\in\mathcal{M}, \quad (21b)$$

$$\sum_{m\in\mathcal{M}}\chi_k(\varpi[m,i_k])+\chi_k(\varpi[i_k,d])=0,\forall i_k\in\mathcal{S}_k, \quad (21c)$$

$$\sum_{m\in\mathcal{M}}\chi_k(\varpi[b,m])=\beta_k(b), \quad (21d)$$

$$\sum_{i_k\in\mathcal{S}_K}\chi_k(\varpi[i_k,d])=\beta_k(d), \quad (21e)$$

$$\beta_k(d)=-\beta_k(b), \quad (21f)$$

where integer $\beta_k(b)\in[0,\min\{M,S_k\}]$ denotes the number of channel-sensor pairs for the k-th application. According to [42], all integral capacities and divergences in the constructed graph make $\mathcal{P}_k$ always have an optimal integer solution, and thus the integrality constraints on the flux of all arcs is considered.

In particular, as shown in (21a), the flow of arc $\chi_k(\varpi[m,i_k])$ indicates whether channel m is allocated to sensor i (belonged to application k) nor not. The flux spread to nodes belonged to set $\mathcal{S}_k$ will not exceed one due to the divergence constraint (21b). It means that $\sum_{i_k\in\mathcal{S}_K}\chi_k(\varpi[m,i_k])\leq 1,\forall m\in\mathcal{M}$, which guarantees that the channel m can be used by at most one sensor belonged to set $\mathcal{S}_k$. Similarly, the node $i_k\in\mathcal{S}_k$ is possible to receive M flux from nodes belonged to set $\mathcal{M}$, but at most one flux can go into the node $i_k\in\mathcal{S}_k$ due to the capacity constraint on the arc $\chi_k(\varpi[i_k,d])$ (21a) and the divergence constraint (21c). In other words, $\sum_{m\in\mathcal{M}}\chi_k(\varpi[m,i_k])\leq 1,\forall i_k\in\mathcal{S}_k$, which restricts that each sensor can obtain at most one channel. The constraints (21d)–(21f) guarantee that the number of channel-sensor pairs for the k-th application will not exceed a threshold (i.e. $\min\{M,S_k\}$).

All above discussions reveal that for each application, (21b) and (21c) in $\mathcal{P}_k$ can satisfy the constraints of orthogonal channel assignment and single channel transmission, i.e., (16a) and (16c) in $\mathcal{P}'_{\{0,1\}}$. Due to the similar objective between (16) and (21), the binary integer programming problem $\mathcal{P}'_{\{0,1\}}$ is equivalent to the minimum flow cost problem $\mathcal{P}_k$. In this regard, the optimal solution of (16) can be obtained by seeking the minimum flow cost through searching the integer $\beta(b)$ in the range of $[0,\min\{M,S_k\}]$. Based on the existing work [24], the optimal integer solution of problem $\mathcal{P}_k$ with certain $\beta(b)\in[0,\min\{M,S_k\}]$ can be obtained by employing the linear optimal distribution algorithm with the complexity $\mathcal{O}((M+S_k+2)^3)$. Therefore, for all possible integer $\beta_k(b)$, the complexity of solving minimum flow problem (21) is no more than $\mathcal{O}(8Z(Z+1)^3)$. In other words, the problem (21) can be optimally solved in polynomial time.

For the general scenario with multiple applications and different-priority sensors deployed for multiple applications, the transmission power of each sensor on the assigned channel can be obtained with the similar procedure for solving problems (10) and (12) under the given channel assignment. Moreover, the updated transmission power can be used to re-handle the channel assignment problem (21).

V. Simulation Results

A. Simulation Scenario and Settings

The considered case study is the hot rolling process, where the dynamic system involved in the temperature estimation application refers to [1]. The considered schemes are evaluated in a star-topology network covering a rectangular area $[0,450]\times[0,50]$, wherein 10 temperature sensors and 13 vibrating sensors are placed, as shown in Fig. 3. All types of sensors share 13 Rayleigh block-fading wireless channels, and the bandwidth of each channel is 200 KHZ. Considering the sensors are powered with battery, the maximum transmit power of each sensor is 10 dBm.

Due to the limitation of transmission power and spectrum resources, this paper employs the ratio of effective throughput and power consumption and the ratio of effective throughput and the number of channels to assess the energy efficiency and the spectrum efficiency, respectively. In the next subsection, the

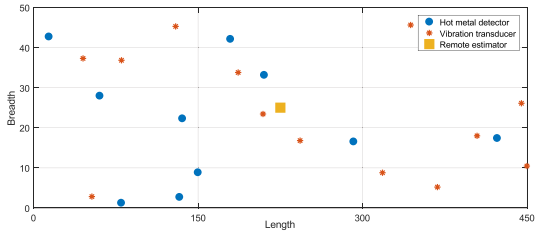

Fig. 3. The network topology of considered hot rolling process.

achieved revenue, energy efficiency and spectrum efficiency are regarded as three main performance metrics.

B. Performance Comparisons

For the purpose comparison, two different transmission schemes are implemented in the following simulations, i.e., the OMA-based on-demand transmission (ODT) scheme and the NOMA-assisted optimal transmission (NOT) scheme with the exhaustive method. For the comparison in the case with multiple applications, the duration of one time slot is divided into K sub-slots and the sensor deployed for each application delivers data packets in one sub-slot. In the TSPT scheme, the fraction of one-slot assigned to the transmission of sensor $i_k\in\mathcal{S}_k,k\in\mathcal{K}$ is denoted by $\rho_{i_k,m}$. Then, the network-wide revenue achieved by sensors on the m-th channel is given by $\mathcal{U}_m^{\text{ODT}}=\sum_{k\in\mathcal{K}}\sum_{i_k\in\mathcal{S}_k}\rho_{i_k,m}\big(R_{i_k}(1-\varepsilon_{i_k,m})-\mu_{i_k,m}p_{i_k,m}\big)$. Taking the maximum transmission power into account, the constrained optimization problem in the OMA mode with given channel assignment is shown as

$$\mathcal{P}_{\text{ODT}}:\max_{\{p,\rho\}}\ \sum_{m\in\mathcal{M}}\mathcal{U}_m^{\text{ODT}} \tag{22}$$

$$s.t. 0\leq\rho_{i_k,m}\leq 1,\forall i\in\mathcal{S}_k,k\in\mathcal{K},\forall m\in\mathcal{M}, \tag{22a}$$

$$\varepsilon_{i_k}\leq\varepsilon_k^{th},\forall i\in\mathcal{S}_k,k\in\mathcal{K}, \tag{22b}$$

$$0\leq p_{i_k,m}\leq p_M,\forall i\in\mathcal{S}_k,k\in\mathcal{K}, \tag{22c}$$

where ε_k^{th} is the allowable maximum outage probability of the k-th application. When $\rho_{i_k,m}$ is given, problem (22) can be solved with the method designed for (11). As $\mathcal{U}_m^{\text{ODT}}$ is monotonic in term of $\rho_{i_k,m}$ with given transmission power, the optimal solution is reached at the bounds of $\rho_{i_k,m}$. In this regard, we solve (22) with each bound of $\rho_{i_k,m}$, and then select the one with maximum $\mathcal{U}_m^{\text{ODT}}$ as the optimal solution. The energy-efficient throughput achieved with the ODT scheme is $\mathcal{U}_m^{\text{ODT}}=\sum_{k\in\mathcal{K}}\sum_{i_k\in\mathcal{S}_k}\delta_{i_k,m}(R_{i_k}-\mu_{i_k,m}p_{i_k,m})$.

1) Performance Comparisons Among Different Schemes: The achieved transmission performance with temperature estimation and equipment-health monitoring applications are shown in Fig. 4. It can be seen that the ratio of efficient throughput and energy consumption achieved with NDT scheme is much larger than that with ODT scheme. This performance improvement comes from the NOMA technique, since it enables one resource block to serve multiple applications and then increases the transmitted data volume.

The energy efficiency comparison among NDT, ODT and NOT schemes is shown in Fig. 5(a). It can be seen that the

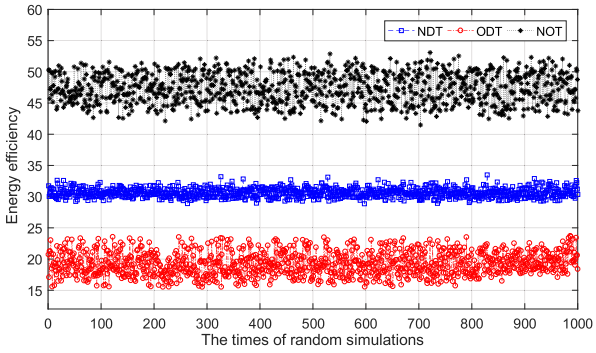

Fig. 4. The energy efficiency comparison among NDT, ODT, and NOT schemes with 1000 random simulations.

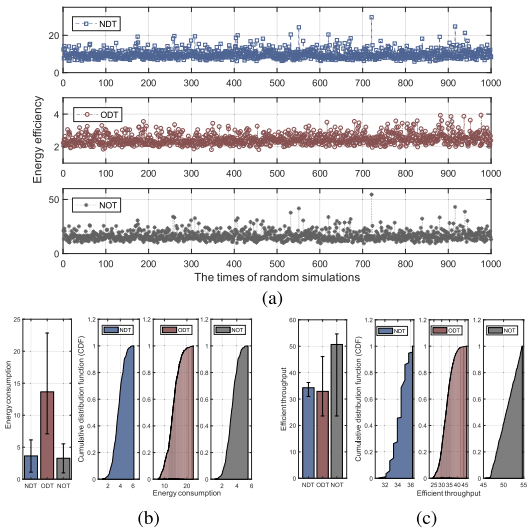

Fig. 5. Transmission performance comparison among different schemes. (a) The energy efficiency with 1000 random simulations. (b) The energy consumption. (c) The efficient throughput.

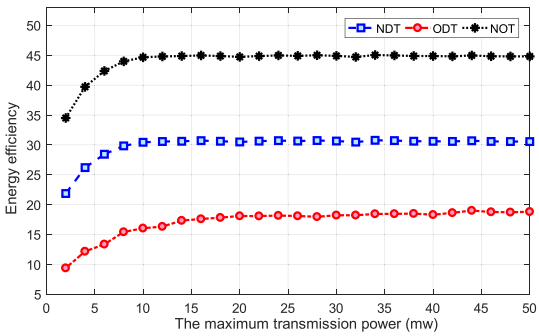

Fig. 6. The energy efficiency with different maximum transmission power.

NOMA has superiority on the energy efficiency than the OMA in time domain. The reason is that the data packet of each sensor can only be delivered in a portion of the duration of one time slot. As a result, the sensor has to increase the transmission power to complete the data-packet transmission within the specific and short duration. The energy consumption of the ODT is significantly larger than those of NDT and NOT schemes, as shown in Fig. 5(b). However, the efficient throughput of ODT is significantly less than those of NDT and NOT schemes, as

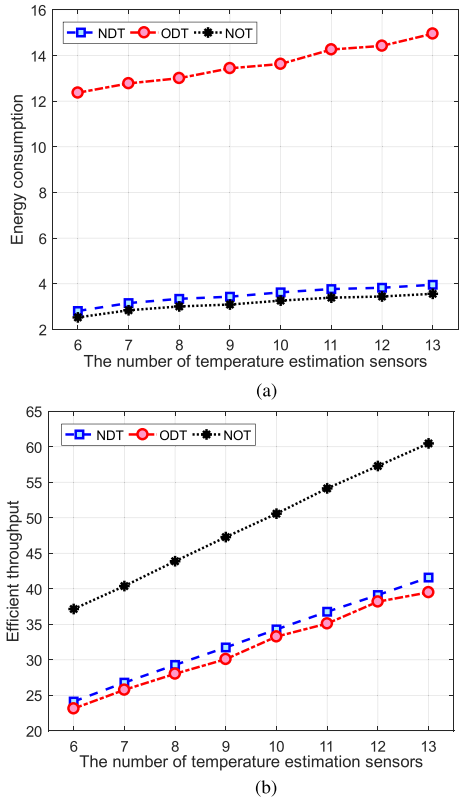

Fig. 7. Transmission performance comparison among different numbers of temperature-estimation sensors. (a) Energy consumption. (b) Efficient throughput.

shown in Fig. 5(c). Therefore, NOMA assisted transmission scheme outperforms the OMA one in both energy efficiency and efficient throughput.

Since the sensors are powered by the batteries, we further show the effect of the maximum transmission power of each sensor on the transmission performance in Fig. 6. It can be seen that with the growth of the maximum transmission power, the network-wide revenues achieved by three schemes will increase and then keep steady at the maximum. The ceiling effect shows that it is impossible to improve the transmission performance by only increasing the transmission power. Therefore, the joint design of channel assignment and power control is of crucial importance to enhance the information transmission performance for industrial monitoring applications.

2) Performance Comparisons With Different Numbers of Sensors and Wireless Channels: The impact of the number of sensors is shown in Fig. 7 and Fig. 8. In particular, Fig. 7(a) and Fig. 7(b) show that energy consumption and efficient throughput increase with the increasing number of sensors. Furthermore, Fig. 8(a) shows that with the increasing of the number of temperature estimation sensors, the variation trends of the network-wide revenues achieved with different schemes are similar. As different channels have diverse channel conditions, the growth of the number of sensors makes some sensors have to work on the relatively worse channels. As a result, larger transmission power will be employed to satisfy the transmission requirement, leading to a decrease in energy efficiency, shown as the blue and black curves in Fig. 8(b). The reason is that for

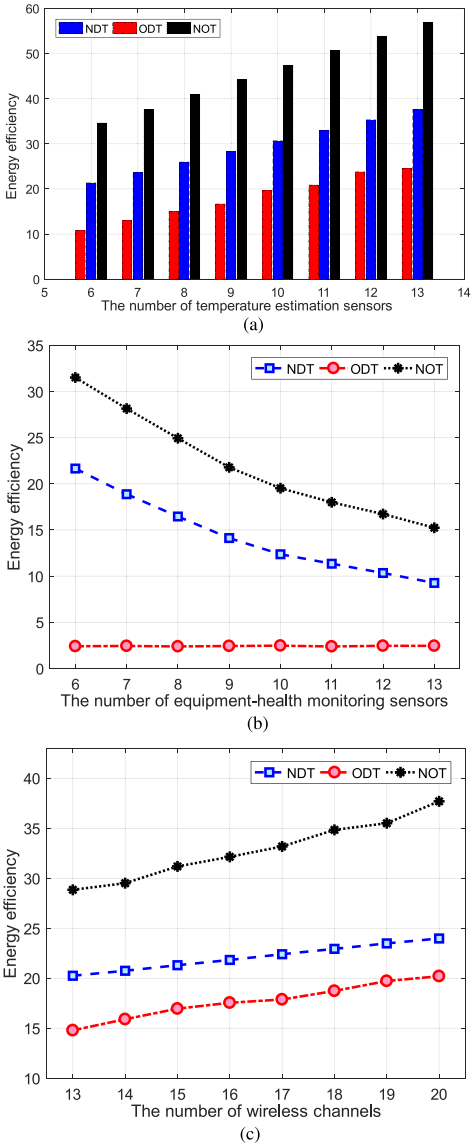

Fig. 8. Transmission performance comparison among different numbers of sensor sand wireless channels. (a) Energy efficiency. (b) Energy efficiency. (c) Energy efficiency.

equipment-health monitoring sensors, the SINR of the received signal is relatively poor due to the co-channel interference from temperature estimation sensors. Furthermore, the lower the SINR is, the less the efficient throughput per power unit is. Therefore, the equipment-health monitoring sensors have to increase the transmission power to improve the effective throughput. Fig. 8(c) shows that the more the channels, the larger the energy efficiency. The reason is that the more channels, the larger probability of selecting better channels as well as the less co-channel interference due to the fewer sensors working on the same channel.

3) Performance Comparisons With Different Numbers of Applications: The performance comparisons among multiple applications are shown in Fig. 9. It can be seen that the achieved energy efficiency with the NDT scheme is larger than that with the ODT scheme but smaller than that with NOT scheme. Furthermore, the application with higher priority can obtain

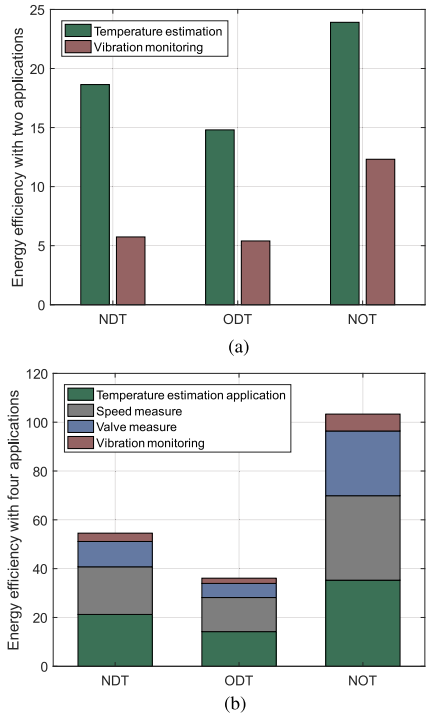

Fig. 9. Energy efficiency with different numbers of applications. (a) Two kinds of applications. (b) Four kinds of applications.

higher transmission performance. In particular, the NOMA-assisted transmission schemes (NDT and NOT), the reason is that the co-channel interferences from sensors deployed for other applications is lower. For the TDMA based transmission scheme (ODT), this result is due to the fact that larger fraction of the transmission duration is assigned to the application with higher priority to satisfy the more stringent performance-quality requirements.

VI. Conclusion

In this paper, the proposed a NOMA assisted on-demand transmission scheme simultaneously guarantee the transmission reliability for the temperature estimation application and improve the sum data rate for equipment-health monitoring applications with limited spectrum resource. Moreover, the proposed scheme has superiorities in improving the energy efficiency for the industrial network with battery-powered sensors. By taking advantage of the heterogenous requirements of different applications, the proposed scheme separates the SIC decoding order from the tight coupling of decoding order, power control and channel assignment, which makes it possible to reduce the design and solution complexity. Furthermore, a mixed integer programming problem is formulated to further improve the scheme performance, which then is solved effectively with the designed the pairwise matching based algorithm and the minimum cost flow based algorithm. Simulation results have demonstrated that the proposed scheme can effectively improve the transmission performance. For our future work, we will investigate both uplink and downlink on-demand transmission scheme for feedback control applications in industrial automation.

REFERENCES

[1] L. Lyu, C. Chen, S. Zhu, and X. Guan, "5G enabled co-design of energy-efficient transmission and estimation for industrial IoT systems," *IEEE Trans. Ind. Inf.*, vol. 14, no. 6, pp. 2690–2704, Jun. 2018.

[2] N. Cheng *et al.*, "Performance analysis of vehicular device-to-device underlay communication," *IEEE Trans. Veh. Technol.*, vol. 66, no. 6, pp. 5409–5421, Jun. 2017.

[3] L. Lyu, C. Chen, J. Yan, F. Lin, C. Hua, and X. Guan, "State estimation oriented wireless transmission for ubiquitous monitoring in industrial cyber-physical systems," *IEEE Trans. Emerg. Topics Comput.*, vol. 7, no. 1, pp. 187–201, Jan.–Mar. 2019.

[4] X. Cao, X. Zhou, L. Liu, and Y. Cheng, "Energy-efficient spectrum sensing for cognitive radio enabled remote state estimation over wireless channels," *IEEE Trans. Wireless Commun.*, vol. 14, no. 4, pp. 2058–2071, Apr. 2014.

[5] Y. Li and L. Cai, "Cooperative device-to-device communication for uplink transmission in cellular system," *IEEE Trans. Wireless Commun.*, vol. 17, no. 6, pp. 3903–3917, Jun. 2018.

[6] H. Zhou, W. Xu, J. Chen, and W. Wang, "Evolutionary V2X technologies toward the internet of vehicles: Challenges and opportunities," *Proc. IEEE*, vol. 108, no. 2, pp. 308–323, Feb. 2020.

[7] Q. Ye and W. Zhuang, "Token-based adaptive MAC for a two-hop internet-of-things enabled MANET," *IEEE Internet Things J.*, vol. 4, no. 5, pp. 1739–1753, Oct. 2017.

[8] H. Zhou *et al.* "WhiteFi infostation: Engineering vehicular media streaming with geolocation database," *IEEE J. Sel. Areas Commun.*, vol. 34, no. 8, pp. 2260–2274, Aug. 2016.

[9] H. Zhou, N. Cheng, Q. Yu, X. S. Shen, D. Shan, and F. Bai, "Toward multi-radio vehicular data piping for dynamic DSRC/TVWS spectrum sharing," *IEEE J. Sel. Areas Commun.*, vol. 34, no. 10, pp. 2575–2588, Oct. 2016.

[10] Q. Ye and W. Zhuang, "Distributed and adaptive medium access control for internet-of-things-enabled mobile networks," *IEEE Internet Things J.*, vol. 4, no. 2, pp. 446–460, Apr. 2016.

[11] H. Zhou *et al.* "Chaincluster: Engineering a cooperative content distribution framework for highway vehicular communications," *IEEE Trans. Intell. Transp. Syst.*, vol. 15, no. 6, pp. 2644–2657, Dec. 2014.

[12] Q. Ye, J. Li, K. Qu, W. Zhuang, X. Shen, and X. Li, "End-to-end quality of service in 5G networks: Examining the effectiveness of a network slicing framework," *IEEE Veh. Technol. Mag.*, vol. 13, no. 2, pp. 65–74, Jun. 2018.

[13] L. Lyu *et al.* "Dynamics-aware and beamforming-assisted transmission for wireless control scheduling," *IEEE Trans. Wireless Commun.*, vol. 17, no. 11, pp. 7677–7690, Nov. 2018.

[14] N. Cheng *et al.* "Big data driven vehicular networks," *IEEE Netw.*, vol. 32, no. 6, pp. 160–167, Nov./Dec. 2018.

[15] H. Zhou, W. Xu, Y. Bi, J. Chen, Q. Yu, and X. Shen, "Toward 5 G spectrum sharing for immersive-experience-driven vehicular communications," *IEEE Wireless Commun.*, vol. 24, no. 6, pp. 30–37, Dec. 2017.

[16] X. Jin *et al.* "A hierarchical data transmission framework for industrial wireless sensor and actuator networks," *IEEE Trans. Ind. Inf.*, vol. 13, no. 4, pp. 2019–2029, Aug. 2017.

[17] D. Yang *et al.* "Assignment of segmented slots enabling reliable real-time transmission in industrial wireless sensor networks," *IEEE Trans. Ind. Electron.*, vol. 62, no. 6, pp. 3966–3977, Jun. 2015.

[18] G. Pocovi, K. I. Pedersen, and P. Mogensen, "Joint link adaptation and scheduling for 5G ultra-reliable low-latency communications," *IEEE Access*, vol. 6, pp. 28 912–28 922, 2018.

[19] S. Verma, Y. Kawamoto, and N. Kato, "Energy-efficient group paging mechanism for qos constrained mobile iot devices over lte-a pro networks under 5G," *IEEE Internet Things J.*, vol. 6, no. 5, pp. 9187–9199, Oct. 2019.

[20] Y. Wu, K. Ni, C. Zhang, L. P. Qian, and D. H. Tsang, "NOMA-assisted multi-access mobile edge computing: A joint optimization of computation offloading and time allocation," *IEEE Trans. Veh. Technol.*, vol. 67, no. 12, pp. 12 244–12 258, Dec. 2018.

[21] D. Zhai, R. Zhang, L. Cai, B. Li, and Y. Jiang, "Energy-efficient user scheduling and power allocation for noma-based wireless networks with massive iot devices," *IEEE Internet Things J.*, vol. 5, no. 3, pp. 1857–1868, Jun. 2018.

[22] Y. Dai, M. Sheng, J. Liu, N. Cheng, X. Shen, and Q. Yang, "Joint mode selection and resource allocation for D2D-enabled NOMA cellular networks," *IEEE Trans. Veh. Technol.*, vol. 68, no. 7, pp. 6721–6733, Jul. 2019.

[23] Z. Shi, W. Gao, S. Zhang, J. Liu, and N. Kato, "AI-enhanced cooperative spectrum sensing for non-orthogonal multiple access," *IEEE Wireless Commun.*, vol. 27, no. 2, pp. 173–179, Apr. 2020.

[24] L. P. Qian, A. Feng, Y. Huang, Y. Wu, B. Ji, and Z. Shi, "Optimal SIC ordering and computation resource allocation in MEC-aware NOMA NB-IoT networks," *IEEE Internet Things J.*, vol. 6, no. 2, pp. 2806–2816, Apr. 2019.

[25] Z. Ding *et al.* "Application of non-orthogonal multiple access in LTE and 5G networks," *IEEE Commun. Mag.*, vol. 55, no. 2, pp. 185–191, Feb. 2017.

[26] A. Zakeri, M. Moltafet, and N. Mokari, "Joint radio resource allocation and sic ordering in NOMA-based networks using submodularity and matching theory," *IEEE Trans. Veh. Technol.*, vol. 68, no. 10, pp. 9761–9773, Oct. 2019.

[27] X. Shao, C. Yang, D. Chen, N. Zhao, and F. R. Yu, "Dynamic IoT device clustering and energy management with hybrid NOMA systems," *IEEE Trans. Ind. Inf.*, vol. 14, no. 10, pp. 4622–4630, Oct. 2018.

[28] Y. Wu, L. P. Qian, H. Mao, X. Yang, H. Zhou, and X. Shen, "Optimal power allocation and scheduling for non-orthogonal multiple access relay-assisted networks," *IEEE Trans. Mobile Comput.*, vol. 17, no. 11, pp. 2591–2606, Nov. 2018.

[29] L. Zhu, J. Zhang, Z. Xiao, X. Cao, D. O. Wu, and X. Xia, "Joint power control and beamforming for uplink non-orthogonal multiple access in 5 G millimeter-wave communications," *IEEE Trans. Wireless Commun.*, vol. 17, no. 11, pp. 6177–6189, Jul. 2018.

[30] W. Shin *et al.* "Coordinated beamforming for multi-cell MIMO-NOMA," *IEEE Commun. Lett.*, vol. 21, no. 1, pp. 84–87, Jan. 2017.

[31] L. P. Qian, Y. Wu, H. Zhou, and X. Shen, "Dynamic cell association for non-orthogonal multiple-access V2S networks," *IEEE J. Sel. Areas Commun.*, vol. 35, no. 10, pp. 2342–2356, Oct. 2017.

[32] P. D. Diamantoulakis, K. N. Pappi, G. K. Karagiannidis, H. Xing, and A. Nallanathan, "Joint downlink/uplink design for wireless powered networks with interference," *IEEE Access*, vol. 5, pp. 1534–1547, 2017.

[33] Z. Zhang, H. Sun, and R. Q. Hu, "Downlink and uplink non-orthogonal multiple access in a dense wireless network," *IEEE J. Sel. Areas Commun.*, vol. 35, no. 12, pp. 2771–2784, Dec. 2017.

[34] L. Lyu, C. Chen, S. Zhu, N. Cheng, B. Yang, and X. Guan, "Control performance aware cooperative transmission in multiloop wireless control systems for industrial IoT applications," *IEEE Internet Things J.*, vol. 5, no. 5, pp. 3954–3966, Oct. 2018.

[35] C. Yang, J. Zheng, X. Ren, W. Yang, H. Shi, and L. Shi, "Multi-sensor Kalman filtering with intermittent measurements," *IEEE Trans. Autom. Control*, vol. 63, no. 3, pp. 797–804, Mar. 2017.

[36] B. Sinopoli, L. Schenato, M. Franceschetti, K. Poolla, M. I. Jordan, and S. S. Sastry, "Kalman filtering with intermittent observations," *IEEE Trans. Autom. Control*, vol. 49, no. 9, pp. 1453–1464, Sep. 2004.

[37] Y. Zhang, H.-M. Wang, T.-X. Zheng, and Q. Yang, "Energy-efficient transmission design in non-orthogonal multiple access," *IEEE Trans. Veh. Technol.*, vol. 66, no. 3, pp. 2852–2857, Mar. 2016.

[38] W. Dinkelbach, "On nonlinear fractional programming," *Manage. Sci.*, vol. 13, no. 7, pp. 492–498, 1967.

[39] J. A. Koupaei, S. M. M. Hosseini, and F. M. Ghaini, "A new optimization algorithm based on chaotic maps and golden section search method," *Eng. Appl. Artif. Intell.*, vol. 50, pp. 201–214, 2016.

[40] M. Mollanoori and M. Ghaderi, "Uplink scheduling in wireless networks with successive interference cancellation," *IEEE Trans. Mobile Comput.*, vol. 13, no. 5, pp. 1132–1144, May 2014.

[41] M. Tao and Y. Liu, "A network flow approach to throughput maximization in cooperative OFDMA networks," *IEEE Trans. Wireless Commun.*, vol. 12, no. 3, pp. 1138–1148, Mar. 2013.

[42] R. T. Rockafellar, *Network Flows and Monotropic Optimization*. Hoboken, NJ, USA: Wiley, 1984.

Ling Lyu (Member, IEEE) received the B.S. degree in telecommunication engineering from Jinlin University, Changchun, China, in 2013, and the Ph.D. degree in control theory and control engineering from Shanghai Jiao Tong University, Shanghai, China, in 2019. She joined Dalian Maritime University, China, in 2019, where she is currently an Associate Professor with the Department of Telecommunication. She is a visiting student with the University of Waterloo, Canada (September 2017–September 2018). Her current research interests include wireless sensor and actuator network and application in industrial automation, the joint design of communication and control in industrial cyber-physical systems, estimation and control over lossy wireless networks, machine type communication enabled reliable transmission in the fifth generation network, resource allocation, energy efficiency.

Cailian Chen (Member, IEEE) received the B.Eng. and M.Eng. degrees in automatic control from Yanshan University, Qinhuangdao, China, in 2000 and 2002, respectively, and the Ph.D. degree in control and systems from the City University of Hong Kong, Hong Kong, in 2006.

She joined the Department of Automation, Shanghai Jiao Tong University, in 2008, as an Associate Professor. She is currently a Full Professor. Before that, she was a Postdoctoral Research Associate with the University of Manchester, U.K. (2006–2008). She was a Visiting Professor with the University of Waterloo, Canada (2013–2014). Her research interests include industrial wireless networks and computational intelligence, and Internet of Vehicles. She has authored three research monographs and more than 100 referred international journal papers. She is the inventor of more than 20 patents. She received the prestigious IEEE Transactions on Fuzzy Systems Outstanding Paper Award in 2008, and Best Paper Award of WCSP17 and YAC18. She won the Second Prize of National Natural Science Award from the State Council of China in 2018, First Prize of Natural Science Award from The Ministry of Education of China in 2006 and 2016, respectively, and First Prize of Technological Invention of Shanghai Municipal, China in 2017. She was honored Changjiang Young Scholar in 2015 and Excellent Young Researcher by NSF of China in 2016.

Prof. Chen has been actively involved in various professional services. She serves as an Associate Editor for the IEEE TRANSACTIONS ON VEHICULAR TECHNOLOGY, *IET Cyber-Physical Systems: Theory and Applications*, *Peer-to-Peer Networking and Applications* (Springer). She also served as a Guest Editor of the IEEE TRANSACTIONS ON VEHICULAR TECHNOLOGY, TPC Chair of ISAS19, Symposium TPC Co-Chair of IEEE Globecom 2016, Track Co-Chair of VTC2016-fall and VTC2020-fall, Workshop Co-Chair of WiOpt18.

Nan Cheng (Member, IEEE) received the Ph.D. degree from the Department of Electrical and Computer Engineering, University of Waterloo, Waterloo, ON, Canada, in 2016, and the B.E. and M.S. degrees from the Department of Electronics and Information Engineering, Tongji University, Shanghai, China, in 2009 and 2012, respectively. He worked as a Postdoctoral Fellow with the Department of Electrical and Computer Engineering, University of Toronto, from 2017 to 2019. He is currently a Professor with State Key Lab of ISN and with the School of Telecommunication Engineering, Xidian University, Shaanxi, China. His current research focuses on B5G/6 G, space-air-ground integrated network, big data in vehicular networks, and self-driving system. His research interests also include performance analysis, MAC, opportunistic communication, and application of AI for vehicular networks.

Shanying Zhu (Member, IEEE) received the B.S. degree in information and computing science from North China University of Water Resources and Electric Power, Zhengzhou, China, in 2006, the M.S. degree in applied mathematics from the Huazhong University of Science and Technology, Wuhan, China, in 2008, and the Ph.D. degree in control theory and control engineering from Shanghai Jiao Tong University, Shanghai, China, in 2013. From 2013 to 2015, he was a Research Fellow with the School of Electrical and Electronic Engineering, Nanyang Technological University, Singapore. He joined Shanghai Jiao Tong University, China, in 2015, where he is currently an Associate Professor with the Department of Automation, School of Electronic Information and Electrical Engineering. His research interests focus on multi-agent systems and wireless sensor networks, particularly in coordination control of mobile robots and distributed detection and estimation in sensor networks and their applications in industrial networks.

Xinping Guan (Fellow, IEEE) received the B.Sc. degree in mathematics from Harbin Normal University, Harbin, China, in 1986, and the Ph.D. degree in control science and engineering from the Harbin Institute of Technology, Harbin, China, in 1999. He is currently a Chair Professor with Shanghai Jiao Tong University, Shanghai, China, where he is currently the Dean of School of Electronic, Information and Electrical Engineering, and the Director of the Key Laboratory of Systems Control and Information Processing, Ministry of Education of China. Before that, he was the Executive Director of Office of Research Management, Shanghai Jiao Tong University, a Full Professor and the Dean of Electrical Engineering, Yanshan University, Qinhuangdao, China. His current research interests cover industrial network systems, smart manufacturing, and underwater networks. He has authored or coauthored five research monographs, more than 200 papers in the IEEE Transactions and other peer-reviewed journals, and numerous conference papers. As a Principal Investigator, he has finished/been working on more than 20 national key projects. He is the leader of the prestigious Innovative Research Team of the National Natural Science Foundation of China (NSFC). He is an Executive Committee Member of Chinese Automation Association Council and the Chinese Artificial Intelligence Association Council. He received the Second Prize of the National Natural Science Award of China in both 2008 and 2018, the First Prize of Natural Science Award from the Ministry of Education of China in both 2006 and 2016. He was the recipient of the IEEE Transactions on Fuzzy Systems Outstanding Paper Award in 2008. He is a National Outstanding Youth honored by NSF of China, Changjiang Scholar by the Ministry of Education of China and State-level Scholar of New Century Bai Qianwan Talent Program of China.

Xuemin (Sherman) Shen (Fellow, IEEE) received the Ph.D. degree in electrical engineering from Rutgers University, New Brunswick, NJ, USA, in 1990.

He is currently a University Professor with the Department of Electrical and Computer Engineering, University of Waterloo, Waterloo, ON, Canada. His research interests focus on network resource management, wireless network security, Internet of Things, 5G and beyond, and vehicular ad hoc and sensor networks. He is an Engineering Institute of Canada Fellow, a Canadian Academy of Engineering Fellow, a Royal Society of Canada Fellow, a Chinese Academy of Engineering Foreign Member, and a Distinguished Lecturer of the IEEE Vehicular Technology Society and Communications Society.

Dr. Shen received the R.A. Fessenden Award in 2019 from IEEE, Canada, Award of Merit from the Federation of Chinese Canadian Professionals (Ontario) presents in 2019, James Evans Avant Garde Award in 2018 from the IEEE Vehicular Technology Society, Joseph LoCicero Award in 2015 and Education Award in 2017 from the IEEE Communications Society, and Technical Recognition Award from Wireless Communications Technical Committee (2019) and AHSN Technical Committee (2013). He has also received the Excellent Graduate Supervision Award in 2006 from the University of Waterloo and the Premiers Research Excellence Award (PREA) in 2003 from the Province of Ontario, Canada. He served as the Technical Program Committee Chair/Co-Chair for the IEEE Globecom16, the IEEE Infocom14, the IEEE VTC10 Fall, the IEEE Globecom07, the Symposia Chair for the IEEE ICC10, and the Chair for the IEEE Communications Society Technical Committee on Wireless Communications. He is the elected IEEE Communications Society Vice President for Technical and Educational Activities, Vice President for Publications, Member-at-Large on the Board of Governors, Chair of the Distinguished Lecturer Selection Committee, Member of IEEE ComSoc Fellow Selection Committee. He was/is the Editor-in-Chief for the IEEE INTERNET OF THINGS JOURNAL, IEEE NETWORK, *IET Communications*, and *Peer-to-Peer Networking and Applications*. He is a registered Professional Engineer of Ontario, Canada.